E08-06-0603 Suter

Supplemental Figures

Figure S1. *Aplysia* Src1 and Src2 belong to two distinct subfamilies of invertebrate Src PTKs

Phylogenetic tree analysis of *Aplysia californica* (Ap) Src1 (green box) and Src2 (red box) together with selected vertebrate and invertebrate Src family kinases. Calculated distance values in parenthesis; scale bar indicates 0.01. *Asterina miniata* (Am) SFK1 (Accession # AAS01045); *Caenorhabditis elegans* (Ce) Src1 (NP_490866); Ce Src2 (NP_493502); *Drosophila melanogaster* (Dm) Src42A (AAF57295); Dm Src64B (P00528); *Ephydatia fluviatilis* (Ef) Src2 (BAB82421); Ef Src45 (BAB82422); *Gallus gallus* (Gg) Fyn (Q05876); Gg Src (P00523); Gg Yes (P09324); *Homo sapiens* (Hs) Fyn (P06241); Hs Src (P12931); Hs Yes (P07947); *Hydra vulgaris* (Hv) STK (P17713); *Monosiga ovata* (Mo) SrcF (BAF02918); *Suberites domuncula* (Sd) SRC1 (AAT67599); Sd SRC2 (AAT67600); *Spongilla lacustris* (Sl) SRK1 (P42686); *Strongylocentrotus purpuratus* (Sp) Src (NP_999783); *Tribolium castaneum* (Tc) Src (XP_969129).

Figure S2. Specificity of *Aplysia* Src1 and Src2 antibodies.

(A) Cell lysates from CHO cells expressing Src1-EGFP, Src1, Src2-EGFP or Src2, plus untransfected control cells were separated on 10% SDS-PAGE and immunoblotted with Src1, Src2, pSrc2 (activated Src2) or Src PY418 antibodies. No cross reactivity between Src1 and Src2 antibodies was observed. The Src PY418 antibody used in previous studies (Suter and Forscher, 2001; Suter *et al.*, 2004) specifically detects active Src2, but not Src1. 50 and 75 kD molecular weight markers are indicated. (B) Each Src1, Src2 and pSrc2 antibody detects a single band with

the appropriate molecular weight in *Aplysia* CNS cell lysates. Antibodies were either not preincubated (-) or with 5 mg/ml peptide in PBS (+). Peptide incubation completely prevented the detection of the respective Src bands. The phosphorylated peptide (phospho) of Src2, but not the non-phosphorylated peptide (non-phospho) blocked the detection of activated Src2. Molecular weight standards are indicated. (C) *Aplysia* CNS tissue was incubated with lysis buffer (untreated) or lysis buffer including 0.1 % DMSO, 25 μM of the Src family-selective inhibitor PP2, or 25 μM PP3 (inactive PP2 analog) for 20 min. Pretreatment with PP2 resulted in a 54 % decrease of relative Src2 activation levels when compared to the untreated samples (n=2; $P<0.005$, asterisk). In addition, the autophosphorylation mutant of Src2 (Y407F) expressed in SYF cells had relative pSrc2 signals that were reduced by 93% when compared to wild type Src (unpublished data). These results suggest that the pSrc2 antibody is a specific tool to detect activated Src2.

Figure S3. Specificity of *Aplysia* Src1 and Src2 antibodies for immunofluorescence

(A-C) Src1-immunolabeling of fixed *Aplysia* growth cones where Src1 antibody was directly applied (A) or preincubated with 5 mg/ml Src1 peptide (B). Src1-signals in the P domain were reduced by 40% after preincubation with Src1 peptide when compared to controls (n=37 growth cones), while no reduction was observed with the Src2 peptide (data not shown). (C) No Src signals were detected when the primary antibody was omitted in the staining. (D-F) Src2-immunolabeling of growth cones where Src2 antibody was directly applied (D) or preincubated with 5 mg/ml Src2 peptide (E). Src2-signals were reduced by 46% after preincubation with Src2 peptide (n=26 growth cones), while no reduction was observed with the Src1 peptide (data not shown). (F) No signals were detected without the primary antibody. (G-I) pSrc2-immunolabeling

of growth cones where the pSrc2 antibody was directly applied (G) or preincubated with 5 mg/ml pSrc2 phospho peptide (H). pSrc2-signals were reduced by 54% after preincubation with pSrc2 phospho peptide (n=6 growth cones), while no reduction was observed with the corresponding non-phospho peptide (data not shown). (I) Again, no signals were detected when the primary antibody was left out. A dashed line in (C), (F) and (I) indicates the leading edge of the growth cone. Bars: 10 μm.

Figure S4. Src2-EGFP construct validation

(A) Schematic of Src1- and Src2-EGFP fusion protein constructs used in the present study. (B, C) Structural modeling of the *Aplysia* Src2-EGFP fusion protein in inactive (B) and active (C) forms based on known structure of a GFP variant (PDB# 1EMM), the inactive (PDB# 2SRC) and active (PDB# 1Y57) structures of human Src without the first 86 N-terminal amino acids. In its inactive state, the SH2 domain interacts with the phosphorylated tail tyrosine, and the SH3 domain interacts with both the SH2 and kinase domains. Structural modeling suggests that the linker is long and flexible enough to allow tail regulation in the presence of the EGFP-tag. (D) Western blot analysis of Src2 activation state of wild type Src2 and various Src2 mutants with and without EGFP-tag after expression in Sf9 cells. Sf9 cell lysates were separated on 10% SDS-PAGE (15 μg of protein per lane) and the same membrane was sequentially probed with rabbit anti-pSrc2 antibody (immunoblot (IB): pSrc2 to detect autophosphorylated Src2), goat anti-Src2 antibody (IB: Src2 to detect total Src2) and mouse anti-α tubulin antibody (IB: tubulin as a loading control). The Src2 activation state was determined as the ratio between the pSrc2 and total Src2 signal. While the membrane-defective (G2A) and kinase dead (K286M) mutants had a significantly reduced activation level, the constitutively active mutant (Y518F) was similar to

wild type Src2, independent of the presence of EGFP-moiety. Molecular weight markers are indicated. (E) Quantification of two independent experiments by densitometry and determination of the pSrc2/total Src2 ratio revealed that the G2A mutant was at 26±0.3% (mean value ± SD, P=0.002, asterisk) and the K286M mutant was at 13±3.9% (P=0.02) of the wild type Src2 activation level, whereas the constitutively active tail mutant was not significantly different from wild type Src2 (P=0.60). Similarly, the EGFP fusion proteins of the G2A and K286M mutants were at 25±2.7% (P=0.02) and 14±4.6% (P=0.02) of the wild type Src2 activation level, respectively, while Src2-EGFP (P=0.76) and the tail mutant Y518F-EGFP (P=0.47) were not significantly different from wild type Src2. The same results were observed when expressing these constructs in SYF cells (unpublished data).

Figure S5. Src1- and Src2-EGFP FRAP

(A) Src1-EGFP FRAP. A 10 μm diameter bleach spot was made in the P domain of a growth cone with a 20 mW 488 nm argon laser for 10 s. Images shown were taken at times indicated: before bleaching, immediately after bleaching (t= 0s), 5s and 40s after bleaching. (B) Src2-EGFP FRAP. Bars: 10 μm. (C-D) FRAP recovery curves of Src1- and Src2-EGFP. Fluorescence intensity values are plotted as % of pre-bleach intensity and are average values plus SEM from 6-8 experiments in each case. Diffusion constants (D) are indicated.

Figure S6. Constitutively active Src2 does not associate with endocytic vesicles

(A) Growth cone expressing Src2 Y518F-EGFP exhibits constitutively active Src2 at the plasma membrane and filopodia tips but not in distinct vesicles undergoing linear motion as observed for wild type Src2 (see related Video 7). Intensity fluctuations observed are most likely due to ruffling activity (Video 7). (B) Timelapse montage (10 sec intervals) of C domain region marked in (A) shows vesicle labeled with Texas Red dextran, but not with Src2 Y518F-EGFP, moving retrogradely in the C domain. Bar in (A): 10 μm.

Supplemental Videos

Video 1.mov

Time lapse movie of Src2-EGFP-expressing growth cone (Figure 4A). Arrowhead points at Src2-positive puncta structure in the T zone moving first anterogradely, then retrogradely. Time compression: 30x. Scale bar: 10 μm.

Video 2.mov

Time lapse movie of Src2-EGFP-expressing growth cone (Figure 4A). Arrowhead points at Src2-positive puncta structure in the P domain moving retrogradely. Time compression: 30x. Scale bar: 10 μm.

Video 3.mov

Time lapse movie of Src2-EGFP-expressing growth cone (Figure 4C). Red arrowhead points at Src2-positive tubulovesicular structure in the C domain moving retrogradely. Time compression: 30x. Scale bar: 10 μm.

Video 4.mov

Time lapse movie of Src2-EGFP and MT dynamics in *Aplysia* growth cone using FSM (Figure 5G). Yellow arrowhead points at Src2-positive puncta structure (green) in the P domain moving retrogradely in concert with a MT speckle (red). Time compression: 30x. Scale bar: 10 μm.

Video 5.mov

Time lapse movie of Src2-EGFP and MT dynamics using FSM (montage in Figure 5H). Src2-positive puncta structure (green) in the P domain moving retrogradely in concert with a MT speckle (red). Time compression: 30x. Scale bar: 1 μm.

Video 6.mov

Time lapse movie of Src2-EGFP-positive tubulovesicular structures in the C domain before (in 0.1% DMSO) and after 1 hour treatment with 5 μM nocodazole. 5 minute duration is shown for both DMSO and nocodazole treatment. Note absence of dynamic Src2-positive organelle, reduced leading edge motility and increased Src2 levels after nocodazole treatment. Time compression: 60x. Scale bar: 10 μm.

Video 7.mov

Time lapse movie of Src2 Y518F-EGFP-expressing growth cone shows constitutively active Src2 is enriched in tips of long filopodia (arrowhead). Note the clear absence of linear movements of distinctly labeled Src2 Y518F-EGFP-positive vesicles in any of the growth cone domains. Time compression: 100x. Scale bar: 10 μm.

Supplemental Table S1. Primers used for cloning of Aplysia Src1 and Src2

A) Degenerate primers used for initial PCR reactions

Function	*Sequence*
Forward primer G130-A138 of chicken Src	5'-GGITAYATYCCITCIAAYTAYGTNGC-3'
Reverse primer F278-N287 of chicken Src	5'-TTCCAIGTICCCATCCAIACYTCICCRAA-3'
Reverse primer E332-M341 of chicken Src	5'-CATRTAYTCIGTIACRATRTARATIGGYTC-3'

B) Primers for 5' and 3' RACE reactions

Function	*Sequence*
Nested 5' Src1 RACE primer	5'-GTGGCGTGGCATCGTCCTTGGCTACATAA-3'
5' Src1 RACE primer	5'-CACGCCGCTCCCAGCTGACAGCACAGG-3'
3' Src1 RACE primer	5'-GGCAACCCTCGCGGAACTTTCCTGGTCAGAG-3'
Nested 3' Src1 RACE primer	5'-GGCCCACCGTCCAGTTCCGAGAGC-3'
Nested 5' Src2 RACE primer	5'-GATCTCCCACTGATCTTTTGTGTTGTACGACAGAC-3'
5' Src2 RACE primer	5'-GGTGTGGTGTTGTTCCAAAGACCCTCCCAAACTTC-3'
3' Src2 RACE primer	5'-CAGTCCGTGATGGAGACACAGTCAAACATTACAGA-3'
Nested 3' Src2 RACE primer	5'-GTCATGGGCAGTTTGGAGAAGTTTGGGAGGG-3'

C) Primers for Src1 and Src2 subcloning into pRAT-EGFP vector

Function	*Sequence*
Forward primer Src1	5'-CTATGCACCGGTCGCCACCATGGGCAACCTGTGCGTGAAAG-3'
Reverse primer Src1	5'-ACTGGCAACCGGTCCTCCTCCTCCTCCACGACTAATATCGTCCATCTC-3'
Forward primer Src2	5'-GTATGCACCGGTCGCCACCATGGGTAACTGCTTCGGGGGA-3'
Reverse primer Src2	5'-ACTGGCAACCGGTCCTCCTCCTCCTCCTCGTATGAAAGAGGCCTCTCT-3'

D) Primers for Src1 and Src2 subcloning into pRAT vector

Function	*Sequence*
Forward primer Src1	5’-CTACTCGAATTCCGCCACCATGGGCAACCTGTGCGTGAAAG-3’
Reverse primer Src1	5’-GCTGCGGGAATTCTCAACGACTAATATCGTCCATCTC-3’
Forward primer Src2	5’-CAAATCCGCGGCGCCACCATGGGTAACTGCTTCGGGG-3’
Reverse primer Src2	5’-GCGTCTCCGCGGTTATCGTATGAAAGAGGCCTCTCT-3’

E) Primers for Src1 and Src2 subcloning into pIZV5-6His vector

Function	*Sequence*
Forward primer Src1	5’-ACACACACTAGTACTCCACCATGGGCAACCTGTGCGTGAAAG-3’
Reverse primer Src1	5’-ATAGATCTCGAGCGACGACTAATATCGTCCATCT-3’
Forward primer Src2	5’-ACACACACTAGTACTCCACCATGGGTAACTGCTTCGGGGGAT-3’
Reverse primer Src2	5’-ATAGATCTCGAGCGTCGTATGAAAGAGGCCTCTC-3’

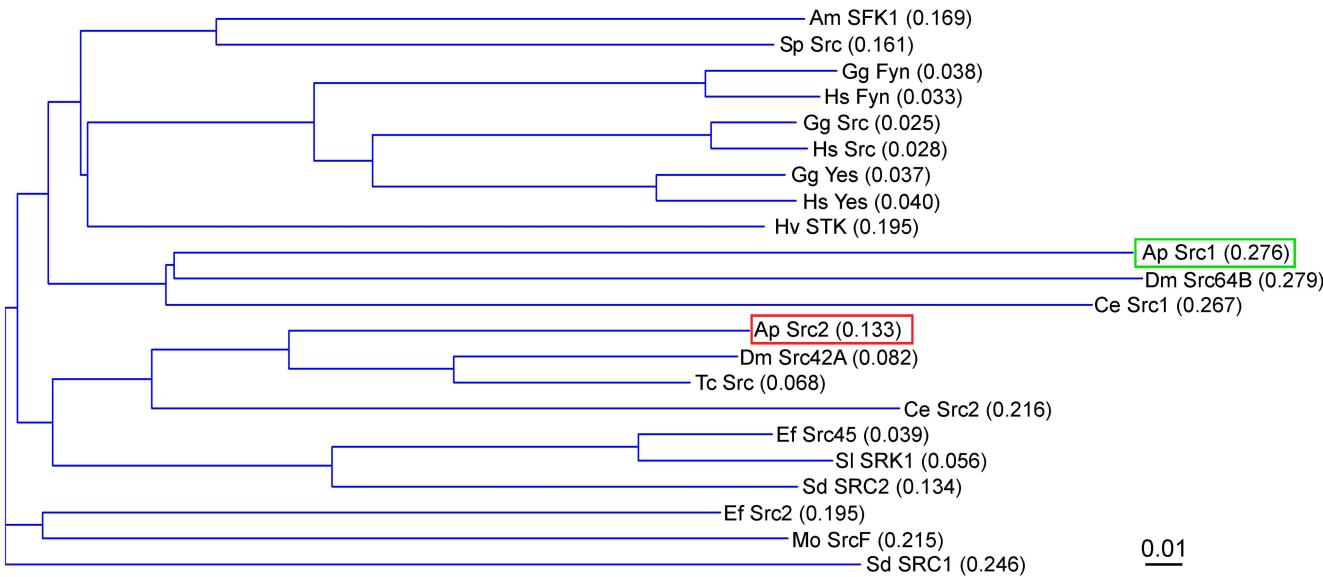

Supplemental Figure S1; Wu et al.

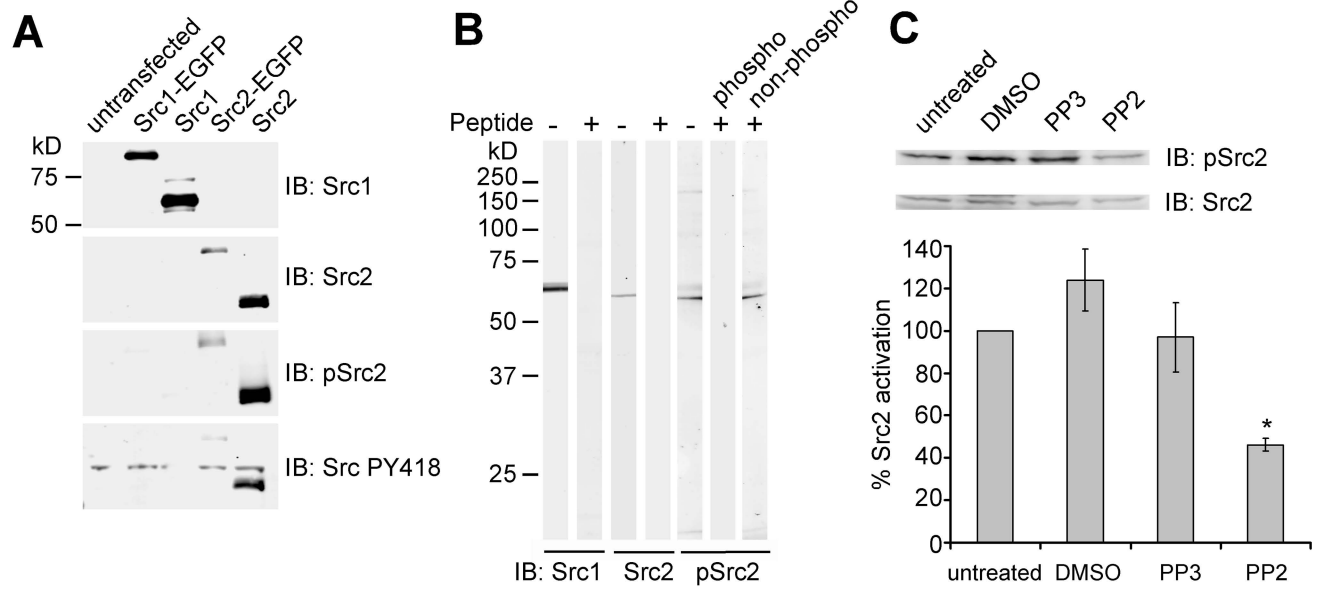

Supplemental Figure S2; Wu et al.

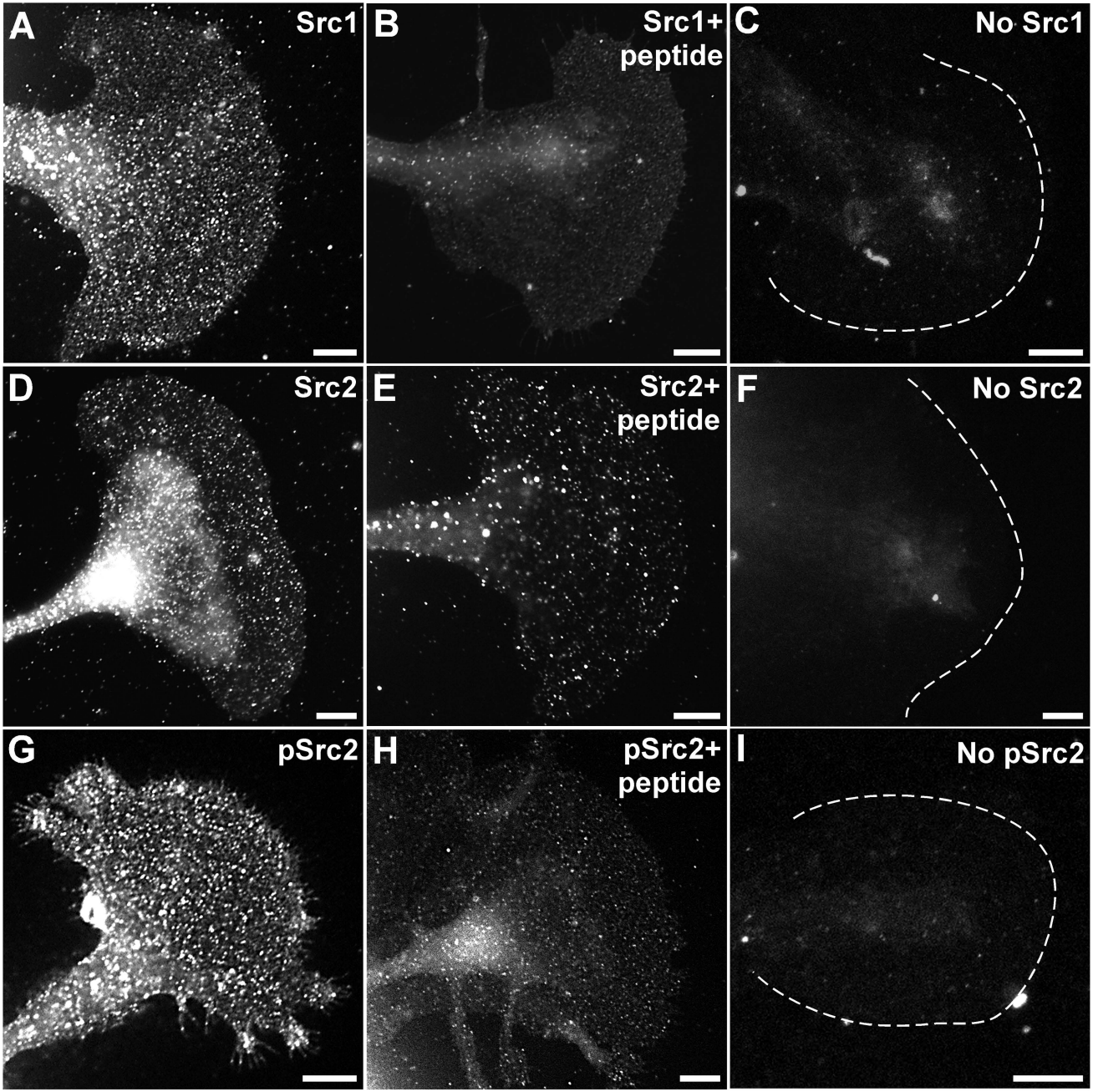

Supplemental Figure S3; Wu et al.

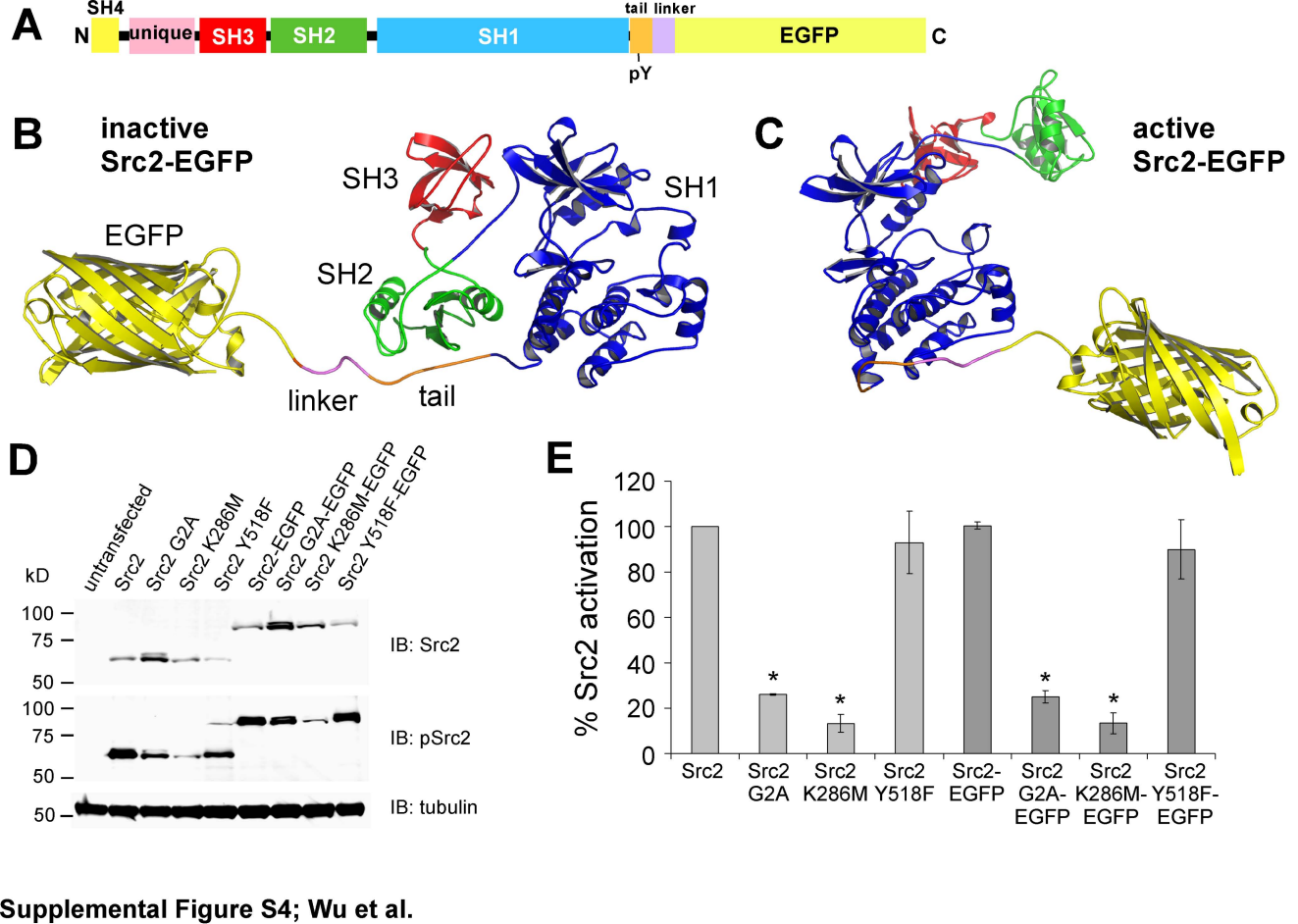

Supplemental Figure S4; Wu et al.

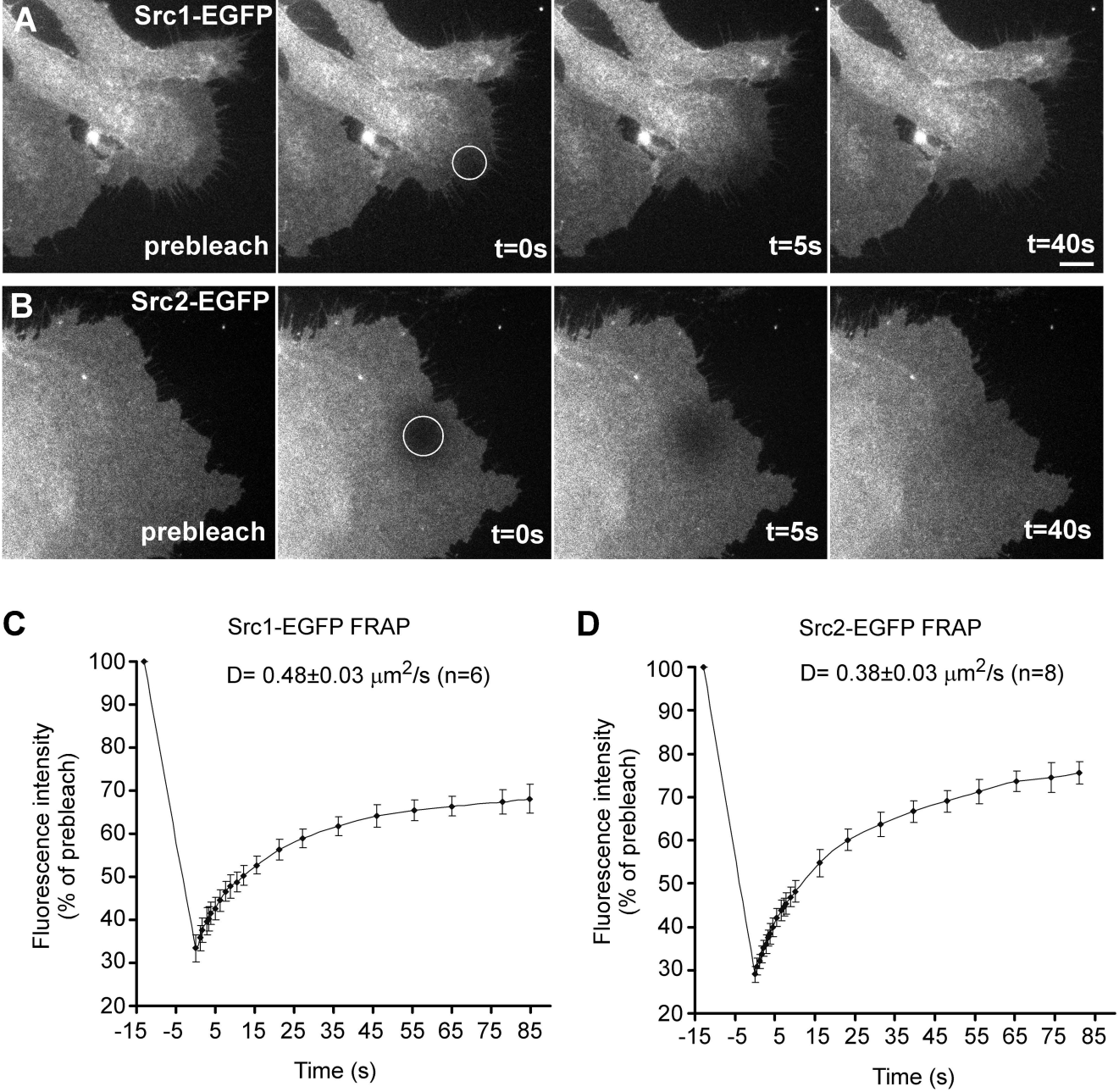

Supplemental Figure S5; Wu et al.

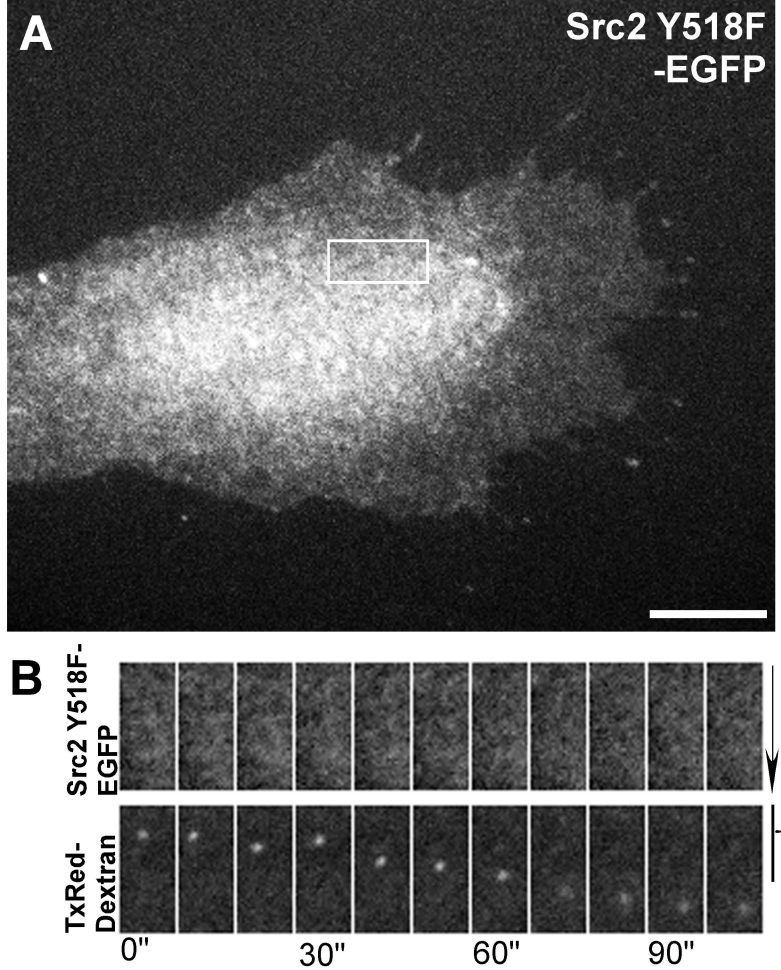

Supplemental Figure S6; Wu et al.